

Adsorbate Orientation Using Angle-Resolved Polarization-Dependent Photoemission*

R. J. Smith, J. Anderson, and G. J. Lapeyre

Montana State University, Bozeman, Montana 59715

(Received 24 May 1976; revised manuscript received 13 September 1976)

Angle-resolved photoemission, using polarized synchrotron radiation, from the system Ni(001)+CO shows two chemisorption peaks which exhibit strong variations in amplitude depending on polar angle of emission and optical polarization. The behavior is in agreement with a recent calculation of angular photoemission from oriented CO molecules, supporting the model of undissociated, "end-on" bonding with the molecular axis perpendicular to the surface, and thus demonstrates that angle-resolved photoemission may give adsorbate geometries.

Several theories of photoemission from adsorbed overlayers^{1,2} have emphasized the potential of polarization- and angle-dependent photoemission experiments for determining important properties of the adsorbed species, e.g., bonding geometry, electron energy levels, and wave-function symmetry. The recent calculations of Davenport³ make specific predictions concerning the amplitude of the photoemission current from an oriented CO molecule; the amplitude is found to depend on photon energy and on the angles, with respect to the molecular axis, of light polarization and electron emission. These predictions may be applied to the case of chemisorbed CO if the only effect of the substrate is to orient the molecule and, possibly, to shift the molecular orbital (MO) energy levels. The purpose of this Letter is to present the observations from our polarization-dependent, angle-resolved photoemission experiment on the chemisorption of CO on Ni(001). We interpret the results in the light of Davenport's calculations according to a model which assumes that (1) the chemisorbed CO molecule is undissociated; (2) the molecules assume a specific orientation with respect to the surface, i.e., the molecular axis is perpendicular to the surface with the carbon atom down; and (3) the 4σ MO wave function is only weakly perturbed by the substrate. The experimental agreement with the predictions of the model supports the end-on bonding configuration, with the carbon atom adjacent to the substrate. We believe that these observations demonstrate, for the first time, the potential of such photoemission measurements, combined with model calculations, for determining adsorbate bonding configurations.

The experiments were performed at the University of Wisconsin Synchrotron Radiation Center. The sample was a thin single crystal (001) Ni ribbon, cleaned *in situ* by Ar⁺ bombardment and subsequent annealing. Surface cleanliness was

monitored by Auger spectroscopy, and photoemission from the clean Ni showed angular anisotropy consistent with a fourfold symmetric surface. The electron analyzer was a cylindrical mirror analyzer, modified for the measurement of emission into arbitrary polar and azimuthal angles, θ_p and φ_p , with 4° angular resolution.⁴ $\theta_p = 0$ is normal to the sample and $\varphi_p = 0$ is the direction of the component of \vec{A} , the vector potential, in the surface plane (see Fig. 1, inset). For s polarization the linearly polarized synchrotron radiation was incident normal to the sample. The

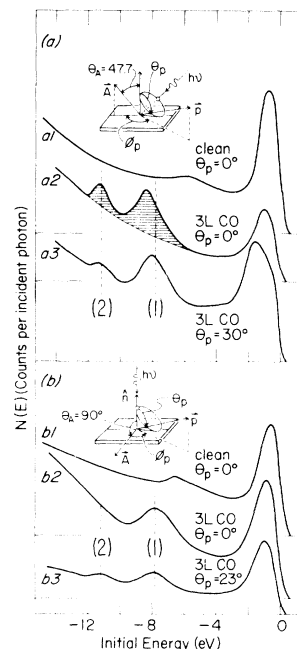


FIG. 1. Angle-resolved energy distribution curves for Ni(001) and Ni(001)+3 L of CO $h\nu = 28$ eV. The inset shows the experimental configuration for (a) nearly p polarization, and (b) s polarization. The curves, plotted as functions of initial energy, are normalized to the incident photon flux as determined from the fluorescence of sodium salicylate.

sample mount could be rotated *in situ* to achieve either *s* or partial *p* polarization.⁵ In the *p* configuration, the angle between \vec{A} and the surface normal was $\theta_A = 47.7^\circ$, and for the *s* configuration $\theta_A = 90^\circ$.

The polarization dependence of the CO emission peaks on Ni(001) is illustrated in Fig. 1 which shows angle-resolved energy distribution curves (AREDC) for photon energy $h\nu = 28$ eV and for various polar angles, θ_p , of emission, with *s* and *p* polarization. The spectra are plotted as functions of initial energy, E_i , below the Fermi energy, E_F . Curves (a1) and (b1) show the normal emission ($\theta_p = 0$) from clean nickel for *p* and *s* polarization, respectively. The dominant peak near E_F has been observed by other investigators⁶ and is attributed to *d*-like bands. The small broad peak at ~ -6 eV may be due to the lower *s-p* band along the symmetry line Δ .⁷ The other four curves show the effects on the AREDC's due to an exposure of 3 L of CO [1 L (Langmuir) = 10^{-6} Torr sec]. In terms of observable photoemission effects, 3 L of CO appeared to saturate the surface at room temperature. The adsorbed CO has some effect on the peak near E_F ; that peak in curve (a2) is reduced by 50%.⁸ However, we wish to focus on the behavior of the two CO peaks, located at $E_i \sim -8$ and -11 eV and labeled (1) and (2), respectively. These are the familiar CO peaks observed in numerous photoemission experiments.^{6,9} By comparison of the properties of these peaks, including their $h\nu$ dependence, with gas-phase emission data,⁹ the following MO assignments have been made: 4σ -derived orbital for peak (2), and a combination of 1π - and 5σ -derived orbitals for peak (1), where the details for the latter combination are still incomplete.

We discuss in detail the behavior of the 4σ -like peak only since it is probably only weakly perturbed by the substrate, at least for linear bonding,¹⁰ and is therefore more amenable to comparisons with a molecular calculation. The major observations for the 4σ -like peak are these: (1) At normal emission ($\theta_p = 0$) the 4σ -like peak is observed with *p* polarization ($\theta_A = 47.7^\circ$) but is not observed with *s* polarization ($\theta_A = 90^\circ$), for all $h\nu \lesssim 40$ eV; (2) for both polarizations the peak is observed for nonnormal emission; and (3) the emission is azimuthally isotropic when the sample is rotated about its normal. The experimental amplitudes plotted in Fig. 2 were obtained as indicated in Fig. 1 by determining the amplitude of the shaded peak above an estimated background of secondaries. The entire data set was then

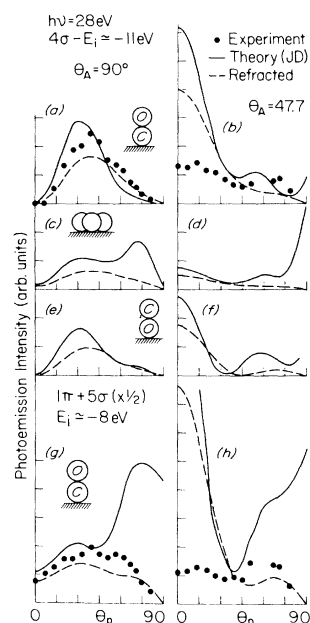


FIG. 2. Calculated photoemission polar intensities for three orientations of a CO molecule for *s*- and *p*-polarized radiation (solid curves). The dashed curves show the possible effects of refraction at the surface, and the filled circles indicate the measured emission peak heights. Panels (g) and (h) are reduced by a factor of 2, relative to the other panels.

scaled by a single constant to give an approximate fit to the 4σ and $1\pi + 5\sigma$ theoretical curves. As pointed out below, the requirement that the -8 -eV emission amplitude be reasonably predicted by the theory is an essential point to our conclusion of linear bonding.

In Fig. 2 the observed polar dependence of the 4σ -like peak is compared with Davenport's calculated photoionization cross section for three orientations of the CO molecule: (1) molecule on end with carbon down [Figs. 2(a) and 2(b)]; (2) molecule on end with oxygen down [Figs. 2(e) and 2(f)]; and (3) molecule on its side and the emission averaged for four orientations of the molecule, differing by a 90° rotation in the surface plane [Figs. 2(c) and 2(d)]. The averaging was done to account for possible domains in the ordered overlayer.¹¹ We also show in each case the predicted electron distribution when the electron undergoes free-electron-like refraction at the surface (dashed lines) using the work function (6 eV) as a surface potential barrier. Although such a model is perhaps too naive, it does suggest how the emission at large polar angles may be modified by refraction.¹² As noted below, best agreement with theory, based on the above-men-

tioned criteria, is found for case (1), providing photoemission verification of the end-on bonding mode.

The theoretical curves of Fig. 2 have been formatted to the experimental geometry as closely as possible. For our detector, as θ_p is increased by moving the electron window around the cylindrical mirror analyzer detection cone, the angle φ_p between \vec{A} and the surface component of electron momentum, $\vec{p}_{||}$, also increases. Davenport's results depend on φ_p and this dependence is included in the curves of Fig. 2. The effect of interference terms in the dipole matrix element when \vec{A} is neither parallel nor perpendicular to the molecular axis is also incorporated in the "Theory" curves of Fig. 2. We have not included effects due to a small component of \vec{A} at right angles to the direction of \vec{A} shown in Fig. 1 and due to the impure polarization of the synchrotron radiation, nor have we considered the refraction of the incident radiation at the solid surface.

In Figs. 2(a) and 2(b), for the molecule on end with C down, we note the following: (1) For *s* polarization the 4σ calculations predict zero amplitude at normal emission with a peak near 30° in agreement with experiment; (2) for *p* polarization the experimental and theoretical 4σ distributions peak in the normal direction although the predicted amplitude near $\theta_p = 0$ is too large; and (3) the -8 -eV CO emission is reasonably well described by the refracted theoretical $1\pi + 5\sigma$ MO curves except for $\theta_p \approx 30^\circ$ with *p* polarization [Figs. 2(g) and 2(h)].

For the molecule on its side [Figs. 2(c) and 2(d)], the predicted 4σ emission is less than for the C atom down, but the refracted distribution could be fitted fairly well by scaling down the experimental points. This would require, however, that the calculation overestimates the -8 -eV peak emission by nearly an order of magnitude which is not expected since the calculations successfully predict the relative peak amplitudes for the gas-phase data.³ In addition, for the molecule on its side, the calculations predict that the normal emission for $\theta_A = 90^\circ$ is 20% of that for $\theta_A = 47.7^\circ$ and a peak of this size should have been observable in the experiment. Allowing for a random orientation of the molecule on its side does not change this discrepancy at normal emission.

Finally, for the molecule on end with O down [Figs. 2(e) and 2(f)] we note the following: (1) For $\theta_A = 47.7^\circ$ the near-zero amplitude predicted for $\theta_p \sim 40^\circ$ was not observed experimentally; and (2) fitting the data with the 4σ theory curve would

again require that the $1\pi + 5\sigma$ curve greatly overestimate the -8 -eV emission amplitude.

The above comparisons have assumed that the observed polar distributions represent direct adsorbate emission, undistorted by substrate backscattering.² As noted earlier, both CO chemisorption features exhibited nearly constant amplitude as the sample was rotated about its normal, keeping θ_p fixed. This suggests that there is very little substrate backscattering which depends on substrate symmetry directions. The lack of substrate-dependent azimuthal effects does not rule out distortions in the polar distributions due to backscattering from an effectively homogeneous substrate plane. Such distortions cannot be separated out experimentally from the direct adsorbate emission and should be considered in any model calculations.

Based on the above comparisons, our observations demonstrate that the utilization of angular resolution and polarized radiation makes possible the investigation of physical properties of chemisorption systems, beyond the determination of electronic energy levels. In particular, if the model employed here is reasonably correct in predicting the angular distribution of emission with respect to the CO molecular axis, then our results verify, with a good degree of confidence, that the molecule is bound with its axis perpendicular to the substrate surface and the C atom down.

We are grateful to J. W. Davenport for providing the detailed results of his calculations prior to publication. We also thank D. W. Lynch for providing the Ni crystals and acknowledge the assistance of the Wisconsin Synchrotron Radiation Center staff and its director, E. M. Rowe. The technical assistance of M. Baldwin and J. Walker was also invaluable.

*Research sponsored by the U. S. Air Force Office of Scientific Research, Air Force Systems Command, under Grant No. 75-2872. The storage ring is supported by National Science Foundation Grant No. DMR 7415089.

¹J. W. Gadzuk, Phys. Rev. B **10**, 5030 (1974).

²A. Liebsch, Phys. Rev. B **13**, 544 (1976).

³J. W. Davenport, Phys. Rev. Lett. **36**, 945 (1976), and private communication.

⁴J. A. Knapp *et al.*, to be published. For $\theta_p > 26^\circ$ the *s*-polarization results were obtained with 12° angular resolution.

⁵For convenience we refer to the experimental configuration as having *p*-polarized radiation. In fact there is a significant *s* component to \vec{A} . In the dipole approximation, neglecting the change in \vec{A} due to refraction at

the surface, only the polar angle, θ_A , is important in Davenport's calculation.

⁶D. E. Eastman and J. K. Cashion, *Phys. Rev. Lett.* **27**, 1520 (1971); P. J. Page and P. M. Williams, *Faraday Discuss.* **58**, 80 (1974).

⁷R. J. Smith, J. Anderson, J. Hermanson, and G. J. Lapeyre, to be published.

⁸The modified shape of the d -band peak in curve (a3) is not due to CO, but rather to the angular dependence of the substrate emission.

⁹T. Gustafsson, E. W. Plummer, D. E. Eastman, and J. L. Freeouf, *Solid State Commun.* **17**, 391 (1975), and references therein.

¹⁰I. P. Batra and P. S. Bagus, *Solid State Commun.* **16**, 1097 (1975); R. V. Kasowski, *Phys. Rev. Lett.* **37**, 219 (1976).

¹¹J. E. Demuth and T. N. Rhodin, *Surf. Sci.* **45**, 249 (1974).

¹²We have found that the background of secondary electrons is described very well by a free-electron-like refraction model [see, for example, G. D. Mahan, *Phys. Rev. B* **2**, 4334 (1970)] using the work function as a surface potential barrier. It is certainly possible however that the surface potential barrier for a CO photoelectron is radically different from that for a bulk secondary electron.

Resonant Excitonic Contributions to Nonlinear Optical Susceptibilities*

H. -h. Chou and George K. Wong†

Physics Department and Materials Research Center, Northwestern University, Evanston, Illinois 60201

(Received 1 June 1976)

We have observed resonant exciton contributions to the nonlinear optical susceptibilities of CdS when the fundamental frequency was tuned through exciton resonances. We show that our data are in good agreement with quantum-mechanical calculations while the anharmonic oscillator model gives incorrect resonance denominators. We also show that selection rules for exciton contributions are different depending on whether the fundamental frequency or generated second-harmonic frequency is in resonance with exciton states.

Exciton contributions to nonlinear optical susceptibilities have been demonstrated in a series of elegant experiments.¹⁻⁴ In particular, resonant exciton contributions to second-order nonlinear susceptibilities d_{ijk} have been measured by Haueisen and Mahr,¹ Parsons, Chen, and Chang,⁵ and more recently by Levine, Miller, and Nordland.⁴ However, in all these experiments exciton contributions were measured in a frequency range where the generated second-harmonic frequency is in resonance with exciton states ($2\hbar\omega$ resonance). In principle, resonant exciton contributions should also exist when the fundamental frequency is near the exciton energy ($\hbar\omega$ resonance). In this Letter, we would like to report the first observation of exciton contributions to d_{ijk} of CdS when the fundamental frequency was swept through A and B exciton resonances. We show that our data can be described well by quantum-mechanical results. The anharmonic oscillator model which worked well for the case of $2\hbar\omega$ resonance gives incorrect resonance denominators for our case. We also show both experimentally and theoretically that depending on whether $\hbar\omega$ or $2\hbar\omega$ is in resonance, the selection rules for exciton contributions are different.

Since in our experiment both the fundamental

and second-harmonic radiations were strongly absorbed by CdS, the second-harmonic power was measured in a reflection geometry. Our experimental arrangement was similar to those described by other authors.⁶ The fundamental radiation was a nitrogen-laser-pumped dye laser. With Coumarin 102 as dye medium, our laser was tunable between 4750 and 4900 Å with a wavelength resolution of about 0.2 Å (50-kW peak power and 5-nsec pulse width). The dye laser beam was focused onto the polished surface of a high purity CdS crystal which was mounted inside a Janis He dewar and at a temperature of about 6°K. To discriminate second-harmonic against fundamental radiation, we used a 2-cm cell of CoSO₄ saturated in water and a half-meter spectrometer. The sample was oriented so that the c axis is in the surface of the crystal. The polarization and propagation direction of the laser beam are shown in the inset of Fig. 1. d_{33} was measured when the polarization was parallel to the c axis and d_{31} was measured when the polarization was perpendicular to the c axis. A polarization rotator was used to achieve the desired polarizations without disturbing the alignment of our system so that the ratio $|d_{33}|/|d_{31}|$ could be measured accurately. To normalize against fluc-